Acta Pharmacologica Sinica (2017) 38: 924–930
 1671-4083/17
www.nature.com/aps

Original Article

Treating breast cancer metastasis with cabazitaxel-loaded polymeric micelles

Tao ZHONG[1], Bin HE[2], Hai-qiang CAO[2], Tao TAN[2], Hai-yan HU[2], Ya-ping LI[2], Zhi-wen ZHANG[2, *]

[1]*College of Pharmacy, Nanchang University, Nanchang 330006, China;* [2]*State Key Laboratory of Drug Research & Center of Pharmaceutics, Shanghai Institute of Materia Medica, Chinese Academy of Sciences, Shanghai 201203, China*

Abstract

Cancer metastasis is the primary cause of high mortality in breast cancer patients. In this study, we loaded an anti-cancer drug, cabazitaxel (CTX), into polymeric micelles (CTX-loaded polymeric micelles, PCMs), and explored their therapeutic efficacy in breast cancer metastasis. The characteristics of PCMs were investigated, and their anti-metastatic efficacy was assessed using *in vitro* and *in vivo* evaluations. PCMs had an average diameter of 50.13±11.96 nm with a CTX encapsulation efficiency of 97.02%±0.97%. PCMs could be effectively internalized into metastatic 4T1 breast cancer cells *in vitro*. CTX (10 ng/mL) or an equivalent concentration in PCMs did not significantly affected the viability of 4T1 cells, but dramatically decreased the cell migration activities. In an orthotopic metastatic breast cancer model, intravenously administered PCMs could be efficiently delivered to the tumor sites, resulting in a 71.6% inhibition of tumor growth and a 93.5% reduction of lung metastases. Taken together, our results verify the anti-metastatic efficacy of PCMs, thus providing an encouraging strategy for treating breast cancer metastasis.

Keywords: micelles; cabazitaxel; cancer metastasis; breast cancer; 4T1 breast cancer cells

Acta Pharmacologica Sinica (2017) 38: 924–930; doi: 10.1038/aps.2017.36; published online 1 May 2017

Introduction

Metastasis causes approximately 90% of breast cancer-related deaths, which is the process by which breast cancer cells spread from the primary tumor to establish colonization at distant organs[1–6]. Breast cancer cells often develop resistance to several treatment approaches, and conventional therapeutic modalities become ineffective in patients with distant metastasis[2–4, 7–11]. Over the past 30 years, there has been little evidence of survival improvement in patients with metastatic breast cancer after adjuvant chemotherapy[2, 12]. Worse yet, cancer cells may evolve to acquire special properties that can promote their metastasis to distant sites[2, 8]. Several approved and commonly used anti-cancer drugs, including paclitaxel and sunitinib, have stimulated breast cancer metastasis in preclinical models[4, 13, 14]. Therefore, it is highly desirable to find new strategies for the effective treatment of breast cancer metastasis.

Cabazitaxel (CTX), a semi-synthetic derivative of a natural taxoid, has been approved by the US Food and Drug Administration (FDA) for the treatment of refractory prostate cancer, especially in patients with resistance to docetaxel-based chemotherapy[15–18]. P-glycoprotein (P-gp), a member of the ATP-binding cassette transporter family of proteins, is responsible for the resistance of taxane in cancer therapy[19–21]. The primary advantage of CTX is its poor affinity to the overexpressed P-gp, thus enabling its clinical efficacy for treating metastatic prostate cancer following docetaxel-based treatments[18]. This advantage provides a promising opportunity for treating breast cancer metastasis, which has been rarely explored in the literature.

Polymeric micelles, a promising drug-delivery nanovector, have attracted increasing attention in treating cancer metastasis[22–26]. Polymeric micelles are self-assembled nanocarriers with a hydrophobic core and poly(ethylene glycol) (PEG) hydrophilic shell, which can effectively be used in a large variety of anticancer drugs and can avoid clearance from the blood circulation[27–31]. Moreover, the nanometer-sized micelles, with sizes of 10–100 nm, can passively accumulate in the tumor site by capitalizing on enhanced permeability and retention (EPR) effects to achieve anti-tumor activities[27, 28, 32]. Small micelles have superior penetration abilities in solid tumors, and they can deliver various chemotherapeutic agents to sites of metastasis after systemic injection[33–35], thus promoting their efficacy in suppressing metastasis of many cancer types.

Herein, we report the use of CTX-loaded polymeric micelles

*To whom correspondence should be addressed.
E-mail zwzhang0125@simm.ac.cn
Received 2016-12-11 Accepted 2017-03-15

(PCMs) to treat breast cancer metastasis. PCMs were prepared from an anticancer drug, CTX, and an amphiphilic polymer of methoxy poly(ethylene glycol)-b-poly(caprolactone) (mPEG-PCL). In this study, the *in vitro* characterization of PCMs was performed, and cellular uptake in metastatic 4T1 breast cancer cells and *in vitro* anti-migration activity were measured. Moreover, the inhibitory effects of PCMs on tumor growth and lung metastasis were assessed in an orthotopic metastatic breast cancer model to verify their effectiveness in treating breast cancer metastasis.

Materials and methods

Materials

The amphiphilic polymer of methoxy poly(ethylene glycol)-b-poly(caprolactone) ($mPEG_{5000}$-PCL_{6500}) was provided by Shanghai Leonchem Company (Shanghai, China). CTX was purchased from Shanghai Chemleader Biomedical Co Ltd (Shanghai, China). Sulforhodamine B (SRB) and IR-780 iodide were supplied by Sigma-Aldrich (Shanghai, China). Hoechst 33342 and phalloidin-FITC were purchased from Beyotime Institute of Biotechnology (Jiangsu, China). The distilled water used in the experiments were purified using the Milli-Q water purification system.

The 4T1 metastatic breast cancer cell line was supported by Shanghai Cell Bank, Chinese Academy of Sciences (CAS). Cells were incubated in culture media consisting of RPMI-1640 mixed with 10% fetal bovine serum (FBS, Gibco) at 37 °C and 5% CO_2 for further measurement.

Female BALB/c nude mice (18–20 g) were ordered from the Shanghai Experimental Animal Center (Shanghai, China). The animals were acclimatized at an animal care facility for at least 3 d prior to the experiment. All animal experiments were performed according to the guidelines approved by the Institutional Animal Care and Use Committee (IACUC) of the Shanghai Institute of Materia Medica, CAS.

Preparation and characterization of PCMs

PCMs were prepared from CTX and mPEG-PCL using a typical film hydration/sonication method. In brief, the accurately weighed mPEG-PCL and CTX were dissolved in methanol and mixed in a round flask. The mixed solution was evaporated until it was dry under reduced pressure to form a thin film in the flask (Heidolph Laborata 4000, Germany). Then, the film was dispersed in 2 mL of purified water, and sonicated with a probe (JYD-650L, Shanghai, China) to prepare the PCMs. The terminal concentration of CTX in the PCMs was approximately 1.0 mg/mL. By contrast, blank micelles of mPEG-PCL were prepared using the same procedure as control.

The size distribution and zeta potential values of PCMs were measured by dynamic light scattering (DLS) on a Malvern Zetasizer Nano ZS 90 instrument (Malvern, UK). Likewise, PCM morphology was visualized under a field emission transmission electronic microscope (FE-TEM, Tecnai G2 F20 S-Twin, FEI) after negative staining with phosphotungstic acid solution (2%, *w/v*, pH 5.5).

The encapsulation efficiency (EE) of CTX in the PCMs and the drug-loading capacity were determined using a high-performance liquid chromatography (HPLC) method. The free drug was separated from the PCMs by an ultrafiltration method (molecular cut-off: 100 000 Da, Millipore) as previously described[36]. The drug level in the filtrate and the PCMs was determined using an Alliance HPLC system (Waters, USA) under the following conditions: column: XBridge (C_{18}, 250 mm×4.6 mm, 5 μm); mobile phase: acetonitrile-water (70:30, *v/v*); flow rate: 1.0 mL/min; and detection wavelength: 230 nm.

The drug release from the PCMs was monitored in phosphate-buffered solution (PBS, pH 7.4). Briefly, 1.0 mL of PCMs was diluted in 5 mL of PBS and incubated at 37 °C under horizontal shaking (100 r/min, HZ-9611k Thermostatic Oscillator, China). At certain time intervals, samples were collected, and the released drug was separated from the PCMs by ultrafiltration and then analyzed by HPLC, as described above.

Cellular uptake

The cellular uptake of the PCMs was measured in a highly metastatic 4T1 breast cancer cell line. PCMs were labeled with the hydrophobic fluorescence dye IR-780 by physical entrapment. Prior to the measurement, the 4T1 cells were grown on round glass coverslips (Ø 10 mm) in 24-well culture plates at 1×10^4 cells/well and cultured overnight. The fluorescently labeled PCMs were added to each well and incubated for 4 h. By contrast, the nuclei were stained with Hoechst 33342, and actins were counterstained with phalloidin-FITC according to the manufacturer's protocols. Afterwards, samples were detected under a laser confocal scanning microscope (LCSM, Fluoview™ FV 1000, Olympus, Japan).

Cell migration assay

The inhibitory effect of the PCMs on cell migration activity was measured using a transwell mediated migration assay. Briefly, 200 μL of FBS-free RPMI-1640 media with 2×10^5 4T1 cells were added to the upper inserts of the transwell (24-well insert, pore size, 8 μm, Costar, USA), while 600 μL of the culture media with 10% FBS were added to the lower chambers as the chemoattractant. Then, CTX solution, PCMs and blank micelles at equivalent doses of CTX were added to the upper and lower chambers with a terminal CTX concentration of 10 ng/mL. At 24 h after the incubation, the migrated cells were stained with crystal violet solution and imaged under a microscope to evaluate the inhibitory effects on cell migration. By contrast, cells without treatment were used as a negative control.

Cell cytotoxicity

To avoid the interference of cytotoxicity on the anti-migration assay, the cell viability of the 4T1 cells was measured with the sulforhodamine B (SRB) assay[37]. Briefly, the 4T1 cells were seeded in 96-well plates at 3×10^3 cells per well and cultured overnight. Then, CTX, PCMs and blank micelles were added to wells at 10 ng/mL CTX or an equivalent concentration. After 24 h, the cell viability was quantified by SRB assay. By contrast, the untreated cells were used as a negative control.

In vivo distribution of PCMs in tumor-bearing mice

The specific tumor targeting of PCMs was measured in tumor-bearing mice. In brief, 100 μL of 4T1 cell suspension (1×10^6 cells) was injected into the right mammary gland of nude mice to induce the orthotopic metastatic breast cancer model. PCMs were fluorescently labeled with hydrophobic IR-780 for *in vivo* imaging. The fluorescently labeled PCMs were intravenously administered to mice at 1.5 mg/kg. At predetermined time intervals, mice were anesthetized and imaged using an *in vivo* imaging system (IVIS Spectrum, Perkin-Elmer). Moreover, at 12 h after injection, mice were autopsied, and the major organs were carefully removed. The *ex vivo* imaging of PCMs was performed.

In vivo therapeutic efficacy on breast cancer metastasis

The therapeutic efficacy of PCMs on tumor growth and metastasis was investigated in an orthotopic metastatic breast cancer model as described above. The tumor-bearing mice were randomly divided into three groups, which were administered with saline, CTX solution (10 mg/kg) or PCMs via tail vein injection. The injections were performed every 3 d, four times in total. To monitor the tumor growth profiles, the width and length of the tumors were measured every 3 d from the first injection. At the end of the experiment, the mice were sacrificed, and the tumor tissues were carefully removed, photographed and weighed to calculate the inhibitory effects on tumor growth. Meanwhile, the lungs from each group were collected and stained with India ink to detect metastatic nodules. Afterwards, the lung tissues were photographed, and the visualized metastatic nodules in each lung were counted. The inhibition of lung metastasis was defined as the average number of metastatic nodules in the PCMs- or the CTX-treated group compared with the number in the saline group.

Statistical analysis

All results are expressed as the mean±standard deviation (SD). Statistical analysis was performed using two-tailed Student's *t*-test. The difference was defined as significant at $P<0.05$ and very significant at $P<0.01$.

Results

Preparation and characterization of PCMs

PCMs were fabricated from an amphiphilic diblock polymer of PCL_{6500}-PEG_{5000} and CTX using the film hydration/sonication method. The particle size distribution of PCMs was measured by DLS analysis, and the morphology was visualized with FE-TEM. The DLS measurements indicated that the PCMs had a hydrodynamic Z-average diameter of 50.13±11.96 nm with a polydispersity index (PDI) of 0.256 (Figure 1A) and zeta potential value of -2.03±0.12 mV. Based on TEM observations, the PCMs were nanometer-sized particles, which were smaller than the DLS measurements (Figure 1B). This difference could be explained by their different states during the measurements. Moreover, the encapsulation efficiency (EE) and drug-loading capacity of the PCMs were evaluated by HPLC analysis. The water-insoluble CTX can be entrapped in polymeric micelles with an EE value of 97.02%±0.97% and drug-loading capacity of 9.73%±0.09%, indicating the efficient encapsulation of CTX in the PCMs. When the PCMs were diluted with phosphate buffer solution (PBS, pH 7.4), the mean diameter barely changed within 24 h. In addition, the cumulative drug release of CTX from the PCMs was less than 5% in PBS (pH 7.4) within 8 h. These results indicated the good stability of the PCMs in PBS (pH 7.4).

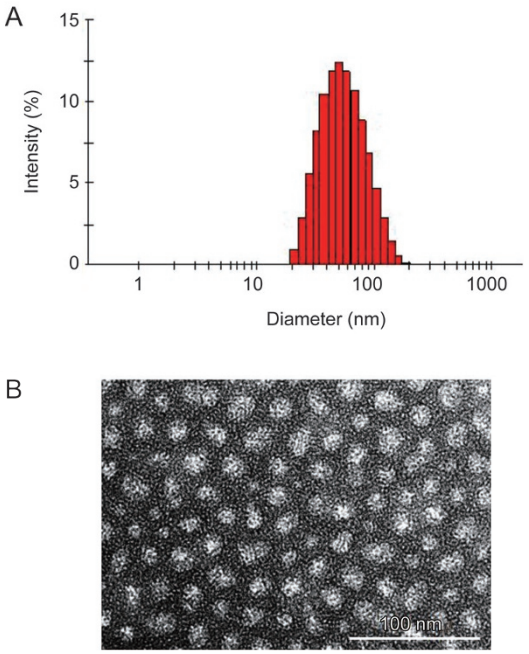

Figure 1. The *in vitro* characterizations of PCM. (A) Particle size distribution of PCM measured by DLS analysis; (B) The typical FE-TEM image of PCM.

In vitro cellular uptake and anti-migration effects

4T1 cells are a highly metastatic breast cancer cell line derived from a mammary tumor of BALB/c mice[38]. The cellular uptake of PCMs in 4T1 cells was visualized under LCSM (Figure 2). PCMs were labeled with hydrophobic fluorescence dye, IR-780, for observation, which was shown as red fluorescence in the captured images. By contrast, the nuclei were stained with Hoechst 33342 (blue), and the actins were stained with phalloidin-FITC (green). As shown in Figure 2, the red fluorescence signals could be extensively observed in 4T1 cells, indicating the efficient uptake of the PCMs into metastatic breast cancer cells.

Then, the inhibitory effects of the PCMs on cell migration were evaluated in metastatic 4T1 breast cancer cells. Prior to the experiments, the cell viability of 4T1 cells treated with CTX and PCMs were evaluated at 10 ng/mL to clarify the possible interference of cytotoxicity on their anti-migration activities. As shown in Figure 3A, the 4T1 cells had high viability at 10 ng/mL CTX or an equivalent concentration in PCMs, which would not interfere with the anti-migration assay. Then, the cell migration activities of 4T1 cells treated with CTX, blank

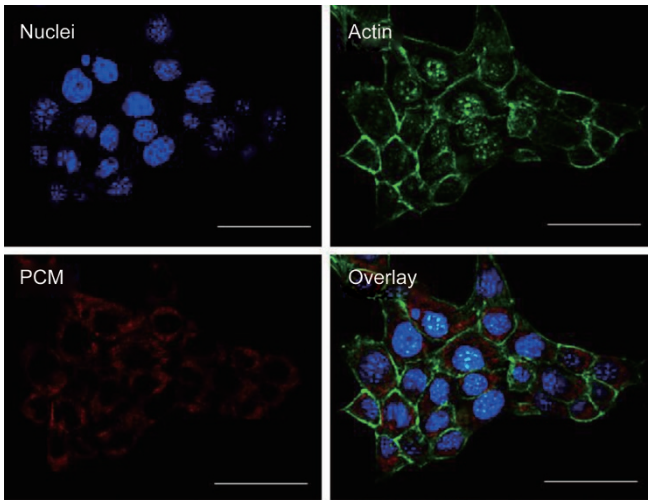

Figure 2. The cellular uptake of PCM in metastatic 4T1 breast cancer cells detected under LCSM, scale bar=50 μm.

micelles and PCMs were evaluated by a transwell mediated cell migration assay (Figure 3B). The images showed many migrated cells in the control group, which confirmed the highly metastatic features of 4T1 cancer cells. When cells were treated with the blank micelles, cell migration was slightly inhibited, which could be attributed to the inhibition effects on ATP[39, 40]. However, in the CTX- and the PCMs-treated groups with 10 ng/mL CTX, only a few cells migrated across the transwell membrane. Compared with the negative control, the percentages of migrated cells in the CTX- and the PCMs-treated groups were only 9.25% and 8.61%, respectively, resulting in more than 90% inhibition of cell migration (Figure 3B). As a result, these experimental results effectively indicated the remarkable effects of CTX and PCMs on inhibiting cell migration activities.

In vivo distribution and therapeutic efficacy

The *in vivo* distribution profiles of the PCMs were monitored in an orthotopic breast cancer model using the *in vivo* imaging system. PCMs were fluorescently labeled with hydrophobic IR-780 for the evaluations. At predetermined time intervals, the fluorescence signals were recorded, and the captured images were shown in Figure 4. The fluorescent signals could be readily detected in tumor sites at different time points after injection, and the fluorescence intensity gradually increased with time up to 8.0 h and then decreased by 12.0 h (Figure 4A). The *ex vivo* images had the strongest fluorescence signals in tumor tissue (Figure 4B). These results effectively verified the specific accumulation of PCMs in tumor sites, which could potentially contribute to the therapeutic efficacy.

The *in vivo* therapeutic efficacy of PCMs on tumor growth and metastasis of breast cancer was evaluated in an orthotopic metastatic breast cancer. In our preliminary experiments, the blank micelles showed minimal cytotoxicity toward 4T1 breast cancer cells. The tumor-bearing mice were treated with saline control, CTX solution or PCMs. In the tumor growth profiles

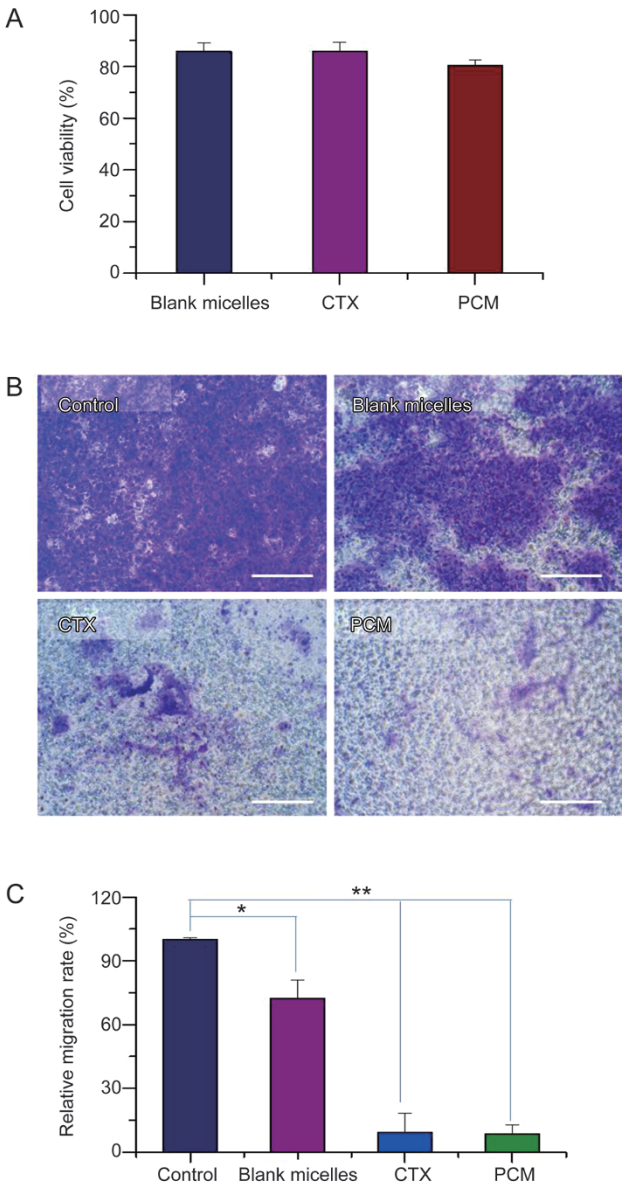

Figure 3. The inhibitory effect of PCM on cell migration activities of metastatic 4T1 breast cancer cells. (A) The cell viability of 4T1 cells treated with blank micelles, CTX and PCM at 10 ng/mL of CTX; (B) Typical images of migrated cells, scale bar=100 μm; (C) Quantification of inhibition effect on cell migration. $^{*}P<0.05$, $^{**}P<0.01$.

(Figure 5A), the tumor volume was progressively increased with time in the saline control group, but it was considerably suppressed in the CTX- and the PCMs-treated groups. Compared with the saline control, the tumor volume on d 24 was 35.5%±6.2% for CTX and 25.8%±5.8% for PCMs, which indicated that both CTX and PCMs effectively inhibited the tumor growth of metastatic breast cancer. At the final time point, the tumor tissues were removed, photographed (Figure 5B), and weighed to calculate the tumor inhibitory rate. As shown in Figure 4C, the tumor weight in the PCMs-treated group was 28.4%±6.4% of the saline group, resulting in a 71.6% inhibi-

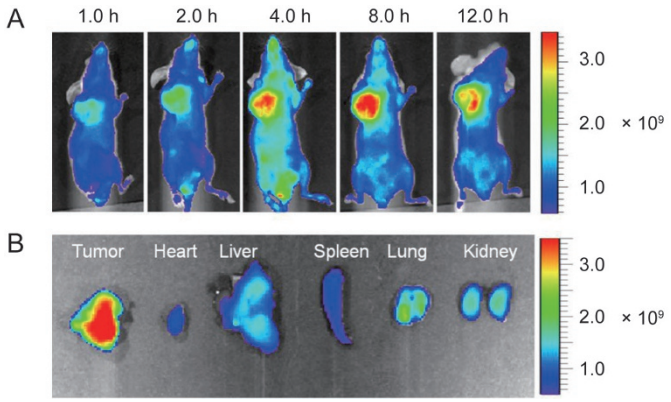

Figure 4. The *in vivo* distribution of PCM in tumor bearing mice. (A) The *in vivo* imaging at different time points; (B) The *ex vivo* imaging of PCM in each major organ.

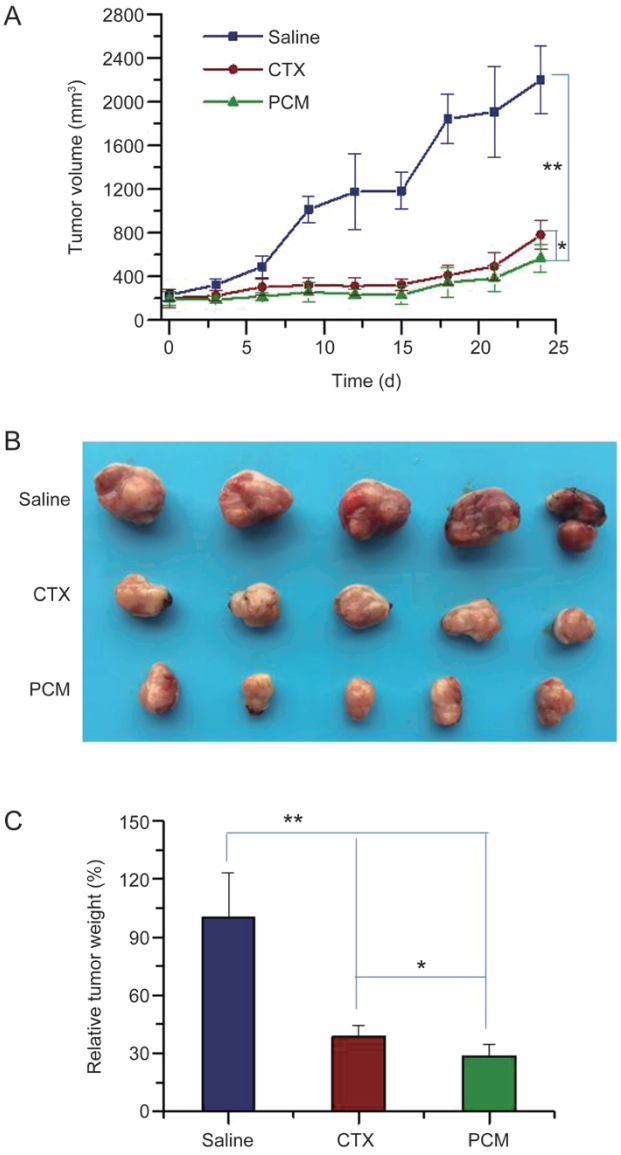

Figure 5. The *in vivo* therapeutic efficacy of PCM on tumor growth of breast cancer model. (A) The tumor growth profiles of 4T1 induced breast cancer model treated with saline, CTX and PCM; (B) The typical images of excised tumor tissues from each group; (C) The relative tumor weight from each group. $^{*}P<0.05$, $^{**}P<0.01$.

tion of tumor growth. In both the tumor growth profiles and tumor weight values, a significant difference was detected between the PCMs- and the CTX-treated groups ($P<0.05$, Figure 5A and 5C), indicating a higher inhibition effect of PCMs on the tumor growth of metastatic breast cancer. The higher inhibition of tumor growth could be due to the specific tumor-targeting ability of PCMs in the tumor-bearing mice.

Moreover, the incidence of lung metastases in metastatic breast cancer was measured to assess the anti-metastasis efficacy. The lung tissues from each group were stained with India ink, and a representative image is shown in Figure 6A. The visualized metastatic nodules in the lungs are denoted as white spots in the captured images. The metastatic nodules could be readily observed in the saline group, but fewer were detected in the CTX- and the PCMs-treated groups (Figure 6A). The numbers of macroscopic metastatic nodules from each group were recorded to evaluate the inhibitory effects on breast cancer lung metastases. Compared with the saline control, the incidence of lung metastases significantly decreased to 13.9% with CTX treatment. The average number of lung metastases from the PCMs-treated group was 4.2±1.5, indicating a 93.5% inhibition of lung metastases (Figure 6B). Moreover, the average number of lung metastases in the PCMs-treated group was only 46.7% of the number in the CTX-treated group ($P<0.05$). The enhanced suppression of the PCMs on the incidence of lung metastasis could be due to the high distribution in lung tissue (Figure 4B). Therefore, PCMs could result in the notable inhibition of lung metastases from breast cancer more effectively than the CTX solution.

Discussion

In the clinic, breast cancer metastasis is the late stage of cancer in which breast cancer cells have disseminated from primary tumor to other parts of the body, such as the lungs, liver, bone and brain[2, 4, 37, 41, 42]. At those locations, they can grow into large aggressive metastatic lesions and directly contribute to the high number of breast cancer-related deaths. Patients with metastatic disease have often been treated with several therapeutic regimens, and the cancer cells have usually developed drug resistance, which can contribute to the ineffectiveness of commonly used chemotherapeutic agents in treating metastatic tumors[2, 7, 8]. Cabazitaxel, which has been synthesized as a dimethyloxy derivative of docetaxel, can eliminate the P-gp affinity characteristics of docetaxel, promoting efficacy against docetaxel-refractory prostate cancer[15, 18]. This primary benefit of CTX would make it attractive for treating breast cancer metastasis. Cell migration activity is directly associated with the ability to metastasize to distant sites[3, 5]. In metastatic 4T1 breast cancer cells, both the CTX solution and the PCMs have remarkable inhibitory effects on cell migration activity. More-

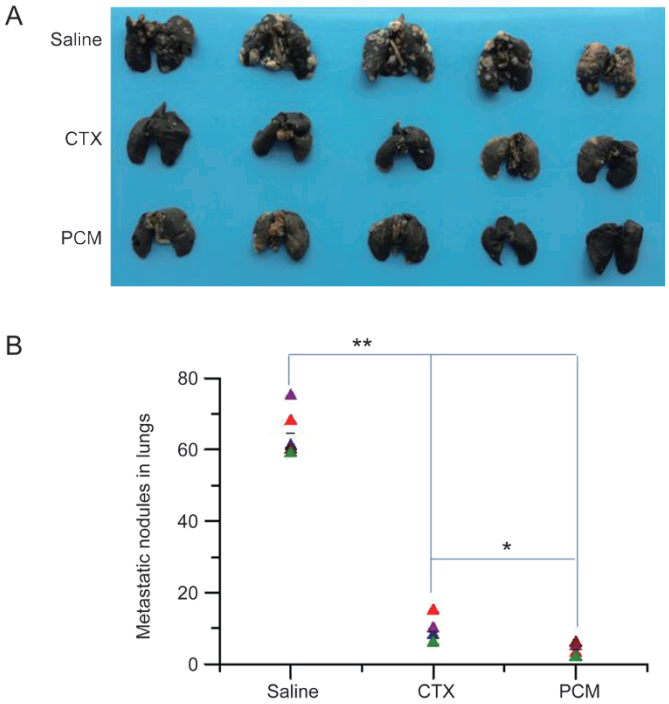

Figure 6. The therapeutic efficacy of PCM on lung metastasis of breast cancer. (A) The typical images of lung metastasis from each group, the metastatic nodules were denoted as white spots in the lung tissues; (B) The number of visualized metastatic nodules in lung tissues from each group. $^{*}P<0.05$, $^{**}P<0.01$.

over, *in vivo* evaluations verified that both the CTX solution and the PCMs have notable inhibitory effects on tumor growth and lung metastases. The anti-metastatic efficacy of the PCMs was significantly higher than that of the CTX solution. These results confirmed the effectiveness of CTX for treating breast cancer metastasis.

In summary, we successfully fabricated CTX-loaded polymeric micelles, which were characterized as nanometer-sized particles with a mean diameter of 50.13±11.96 nm and an encapsulation efficiency of 97.02%±0.97%. PCMs were effectively taken up by metastatic 4T1 breast cancer cells and then considerably inhibited cell migration activities. Moreover, in the orthotopic metastatic breast cancer model, PCMs efficiently accumulated in the tumor sites after injection. Treatment with PCMs resulted in a 71.6% inhibition of tumor growth and a 93.5% suppression of lung metastases. Therefore, the use of CTX-loaded polymeric micelles is an encouraging strategy for treating breast cancer metastasis.

Acknowledgements

This work was supported by the National Basic Research Program of China (No 2013CB932503, 2015CB932103), National Natural Science Foundation of China (No 81521005), Institutes for Drug Discovery and Development of CAS (No CASIMM0120163005) and Youth Innovation Promotion Association of CAS.

References

1 Brabletz T, Lyden D, Steeg PS, Werb Z. Roadblocks to translational advances on metastasis research. Nat Med 2013; 19: 1104–9.
2 Steeg PS. Targeting metastasis. Nat Rev Cancer 2016; 16: 201–18.
3 Wan LL, Pantel K, Kang YB. Tumor metastasis: moving new biological insights into the clinic. Nat Med 2013; 19: 1450–64.
4 Schroeder A, Heller DA, Winslow MM, Dahlman JE, Pratt GW, Langer R, *et al.* Treating metastatic cancer with nanotechnology. Nat Rev Cancer 2012; 12: 39–50.
5 van Denderen BJ, Thompson EW. Cancer: The to and fro of tumour spread. Nature 2013; 493: 487–8.
6 Sahai E. Illuminating the metastatic process. Nat Rev Cancer 2007; 7: 737–49.
7 Eckhardt BL, Francis PA, Parker BS, Anderson RL. Strategies for the discovery and development of therapies for metastatic breast cancer. Nat Rev Drug Discov 2012; 11: 479–97.
8 Fernandez Y, Cueva J, Palomo AG, Ramos M, de Juan A, Calvo L, *et al.* Novel therapeutic approaches to the treatment of metastatic breast cancer. Cancer Treat Rev 2010; 36: 33–42.
9 Niraula S, Ocana A. Mechanism of drug resistance in relation to site of metastasis: Meta-analyses of randomized controlled trials in advanced breast cancer according to anticancer strategy. Cancer Treat Rev 2016; 50: 168–74.
10 Gu W, Dong N, Wang P, Shi C, Yang J, Wang J. Tamoxifen resistance and metastasis of human breast cancer cells were mediated by the membrane-associated estrogen receptor ER-alpha36 signaling *in vitro*. Cell Biol Toxicol 2017, 33: 183–95.
11 Guerrero-Zotano A, Mayer IA, Arteaga CL. PI3K/AKT/mTOR: role in breast cancer progression, drug resistance, and treatment. Cancer Metastasis Rev 2016; 35: 515–24.
12 Tevaarwerk AJ, Gray RJ, Schneider BP, Smith ML, Wagner LI, Fetting JH, *et al.* Survival in patients with metastatic recurrent breast cancer after adjuvant chemotherapy: little evidence of improvement over the past 30 years. Cancer 2013; 119: 1140–8.
13 Volk-Draper L, Hall K, Griggs C, Rajput S, Kohio P, DeNardo D, *et al.* Paclitaxel therapy promotes breast cancer metastasis in a TLR4-dependent manner. Cancer Res 2014; 74: 5421–34.
14 Guerin E, Man S, Xu P, Kerbel RS. A model of postsurgical advanced metastatic breast cancer more accurately replicates the clinical efficacy of antiangiogenic drugs. Cancer Res 2013; 73: 2743–8.
15 Lorente D, Mateo J, Perez-Lopez R, de Bono JS, Attard G. Sequencing of agents in castration-resistant prostate cancer. Lancet Oncol 2015; 16: e279–92.
16 Body JJ, Casimiro S, Costa L. Targeting bone metastases in prostate cancer: improving clinical outcome. Nat Rev Urol 2015; 12: 340–56.
17 Vrignaud P, Semiond D, Lejeune P, Bouchard H, Calvet L, Combeau C, *et al.* Preclinical antitumor activity of cabazitaxel, a semisynthetic taxane active in taxane-resistant tumors. Clin Cancer Res 2013; 19: 2973–83.
18 Paller CJ, Antonarakis ES. Cabazitaxel: a novel second-line treatment for metastatic castration-resistant prostate cancer. Drug Des Devel Ther 2011; 5: 117–24.
19 Zhang Z, Liu Z, Ma L, Jiang S, Wang Y, Yu H, *et al.* Reversal of multidrug resistance by mitochondrial targeted self-assembled nanocarrier based on stearylamine. Mol Pharm 2013; 10: 2426–34.
20 Gottesman MM, Fojo T, Bates SE. Multidrug resistance in cancer: role of ATP-dependent transporters. Nat Rev Cancer 2002; 2: 48–58.
21 Bu H, He X, Zhang Z, Yin Q, Yu H, Li Y. A TPGS-incorporating nanoemulsion of paclitaxel circumvents drug resistance in breast cancer. Int J Pharm 2014; 471: 206–13.
22 He XY, Bao XY, Cao HQ, Zhang ZW, Yin Q, Gu WW, *et al.* Tumor-

penetrating nanotherapeutics loading a near-infrared probe inhibit growth and metastasis of breast cancer. Adv Funct Mater 2015; 25: 2831–9.
23 He XY, Yu HJ, Bao XY, Cao HQ, Yin Q, Zhang ZW*, et al.* pH-Responsive wormlike micelles with sequential metastasis targeting inhibit lung metastasis of breast cancer. Adv Healthc Mater 2016; 5: 439–48.
24 Dan ZL, Cao HQ, He XY, Zhang ZW, Zou LL, Zeng LJ*, et al.* A pH-responsive host-guest nanosystem loading succinobucol suppresses lung metastasis of breast cancer. Theranostics 2016; 6: 435–45.
25 Wu H, Cabral H, Toh K, Mi P, Chen YC, Matsumoto Y*, et al.* Polymeric micelles loaded with platinum anticancer drugs target preangiogenic micrometastatic niches associated with inflammation. J Control Release 2014; 189: 1–10.
26 Sun HP, Su JH, Meng QS, Yin Q, Zhang ZW, Yu HJ*, et al.* Silibinin and indocyanine green-loaded nanoparticles inhibit the growth and metastasis of mammalian breast cancer cells *in vitro*. Acta Pharmacol Sin 2016; 37: 941–9.
27 Gong J, Chen M, Zheng Y, Wang S, Wang Y. Polymeric micelles drug delivery system in oncology. J Control Release 2012; 159: 312–23.
28 Mura S, Nicolas J, Couvreur P. Stimuli-responsive nanocarriers for drug delivery. Nat Mater 2013; 12: 991–1003.
29 Jin ZH, Jin MJ, Jiang CG, Yin XZ, Jin SX, Quan XQ*, et al.* Evaluation of doxorubicin-loaded pH-sensitive polymeric micelle release from tumor blood vessels and anticancer efficacy using a dorsal skin-fold window chamber model. Acta Pharmacol Sin 2014; 35: 839–45.
30 Liu JP, Wang TT, Wang DG, Dong AJ, Li YP, Yu HJ. Smart nanoparticles improve therapy for drug-resistant tumors by overcoming pathophysiological barriers. Acta Pharmacol Sin 2017; 38: 1–8.
31 Zhu JJ, Zhang XX, Miao YQ, He SF, Tian DM, Yao XS*, et al.* Delivery of acetylthevetin B, an antitumor cardiac glycoside, using polymeric micelles for enhanced therapeutic efficacy against lung cancer cells. Acta Pharmacol Sin 2017; 38: 290–300.
32 Ernsting MJ, Murakami M, Roy A, Li SD. Factors controlling the pharmacokinetics, biodistribution and intratumoral penetration of nanoparticles. J Control Release 2013; 172: 782–94.
33 Chauhan VP, Stylianopoulos T, Martin JD, Popovic Z, Chen O, Kamoun WS*, et al.* Normalization of tumour blood vessels improves the delivery of nanomedicines in a size-dependent manner. Nat Nanotechnol 2012; 7: 383–8.
34 Qin L, Zhang FY, Lu XY, Wei XL, Wang J, Fang XC*, et al.* Polymeric micelles for enhanced lymphatic drug delivery to treat metastatic tumors. J Control Release 2013; 171: 133–42.
35 Cabral H, Makino J, Matsumoto Y, Mi P, Wu HL, Nomoto T*, et al.* Systemic targeting of lymph node metastasis through the blood vascular system by using size-controlled nano carriers. ACS Nano 2015; 9: 4957–67.
36 Qu N, Lee RJ, Sun YT, Cai GS, Wang JY, Wang MQ*, et al.* Cabazitaxel-loaded human serum albumin nanoparticles as a therapeutic agent against prostate cancer. Int J Nanomed 2016; 11: 3451–9.
37 Cao H, Dan Z, He X, Zhang Z, Yu H, Yin Q*, et al.* Liposomes coated with isolated macrophage membrane can target lung metastasis of breast cancer. ACS Nano 2016; 10: 7738–48.
38 Zhang ZW, Cao HQ, Jiang SJ, Liu ZY, He XY, Yu HJ*, et al.* Nanoassembly of probucol enables novel therapeutic efficacy in the suppression of lung metastasis of breast cancer. Small 2014; 10: 4735–45.
39 Wang Y, Hao J, Li Y, Zhang Z, Sha X, Han L*, et al.* Poly(caprolactone)-modified Pluronic P105 micelles for reversal of paclitaxcel-resistance in SKOV-3 tumors. Biomaterials 2012; 33: 4741–51.
40 Yao J, Yao X, Tian T, Fu X, Wang W, Li S*, et al.* ABCB5-ZEB1 axis promotes invasion and metastasis in breast cancer cells. Oncol Res 2017; 25: 305–16.
41 Al-Rawi MA, Jiang WG. Lymphangiogenesis and cancer metastasis. Front Biosci 2011; 16: 723–39.
42 Cao HQ, Zhang ZW, Zhao S, He XY, Yu HJ, Yin Q*, et al.* Hydrophobic interaction mediating self-assembled nanoparticles of succinobucol suppress lung metastasis of breast cancer by inhibition of VCAM-1 expression. J Control Release 2015; 205: 162–71.